PNAS
www.pnas.org

Supplementary Information for

Glioblastomas exploit truncated *O*-linked glycans for local and distant immune modulation via the macrophage galactose-type lectin

Sophie A. Dusoswa[a, b], Jan Verhoeff[a, 1], Erik Abels[c, 1], Santiago P. Méndez-Huergo[d], Diego O. Croci[d, e], Lisan H. Kuijper[a], Elena de Miguel[a], Valerie M.C.J. Wouters[a], Myron G. Best[b, f], Ernesto Rodriguez[a], Lenneke A.M. Cornelissen[a], Sandra J. van Vliet[a], Pieter Wesseling[f], Xandra O. Breakefield[c], David P. Noske[b], Thomas Würdinger[b, c], Marike L.D. Broekman[c, g, h], Gabriel A. Rabinovich[d, i, 2], Yvette van Kooyk[a], Juan J. Garcia-Vallejo[a, 2].

Juan J. Garcia-Vallejo
E-mail: jj.garciavallejo@amsterdamumc.nl

Gabriel A. Rabinovich
Email: gabyrabi@gmail.com

This PDF file includes:

Supplementary text
Figs. S1 to S8
Tables S1 to S2

Other supplementary materials for this manuscript include the following:

Datasets S1

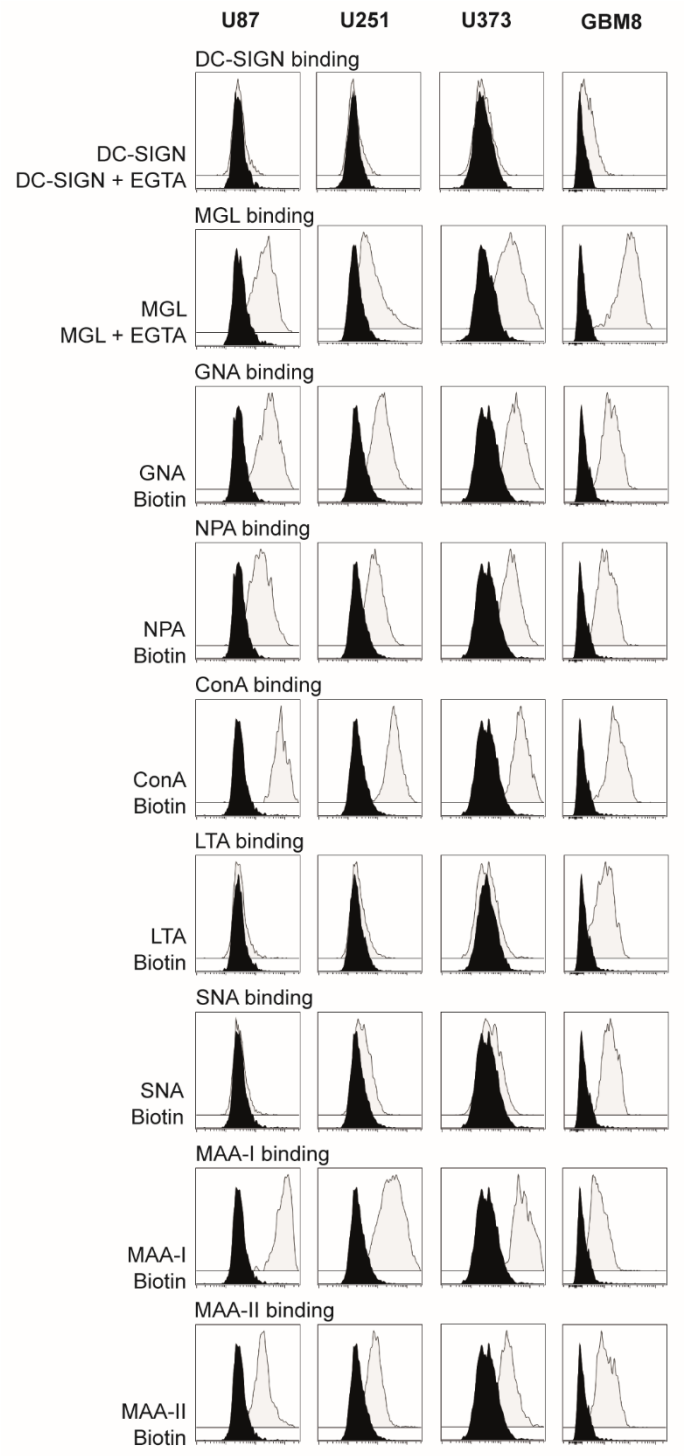

Fig. S1. Lectin binding screen. Overlayed histograms, representative for N=3, showing lectin binding versus a negative controls which include added EGTA in the case of the human lectins DC-SIGN and MGL to prevent calcium dependent binding and the secondary only control (AlexaFluor488/ labelled streptavidin) for the other lectins.

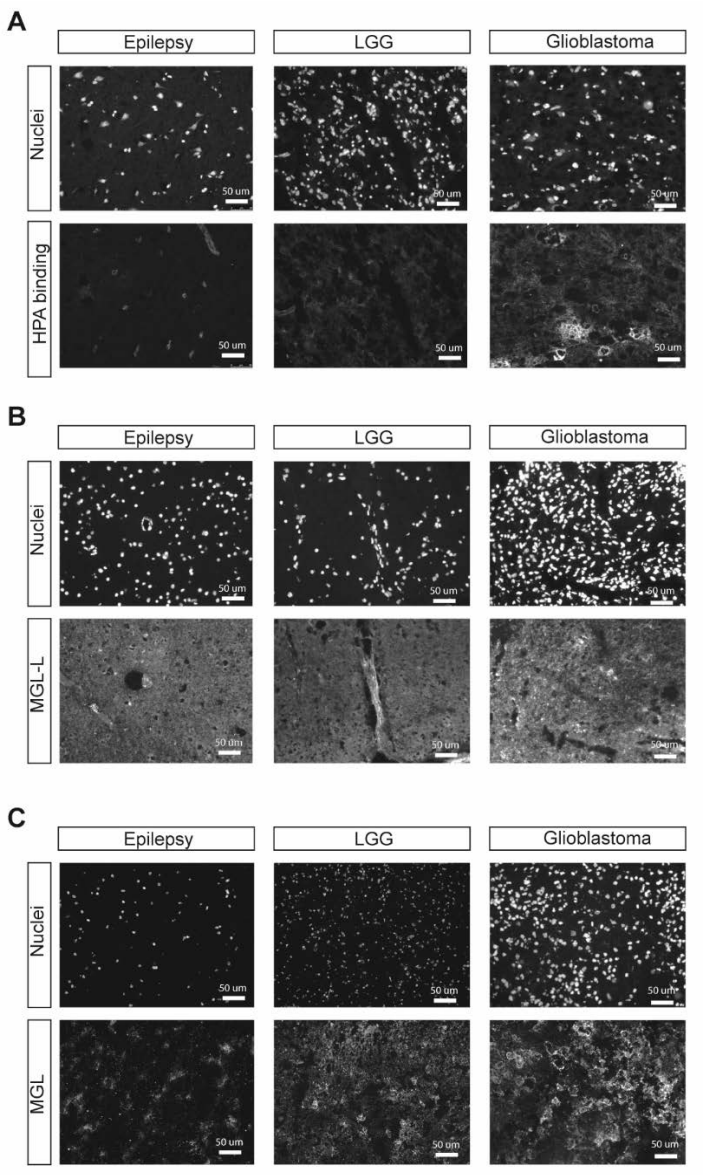

Fig. S2. Immunofluorescence single channels. Seven µm cryosections of surgical epilepsy, LGG, and glioblastoma (GBM) samples, representative for 5 patients per condition, stained with **a.** HPA (green) and Hoechst as nuclear counterstain (blue), **b.** MGL-mouseFc (red) and Hoechst as nuclear counterstain (blue), and **c.** the MGL receptor (yellow) and nuclei (blue).

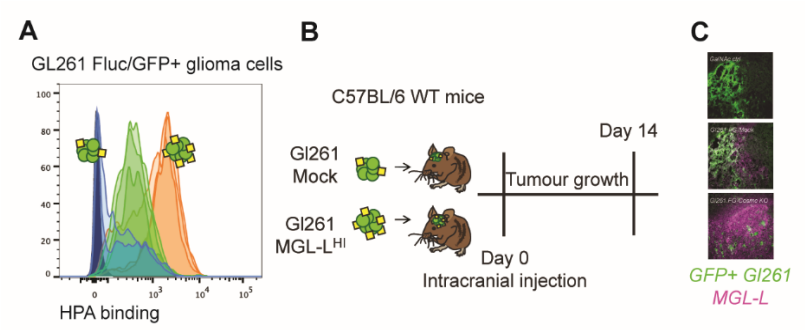

Fig. S3. Murine model for MGL-L^{HI} glioblastoma. a. Expression of immature *O*-linked glycans on MGL-L^{Hi} cells and WT cells, shown by HPA binding and measured by flow cytometry. **b.** A schematic representation of the setup of the *in vivo* experiment with the aim to study the stability of the MGL-L^{Hi} phenotype. **c.** Immunofluorescence showing murine MGL2 binding (purple) to tissues with GFP^{+} MGL-L^{Hi} tumours (green, lower panel) compared to tissues with GFP^{+} WT tumours (middle panel). In the GalNAc control (upper panel), MGL2 was pre-incubated with its natural ligand GalNAc to exclude Fc-tail mediated binding.

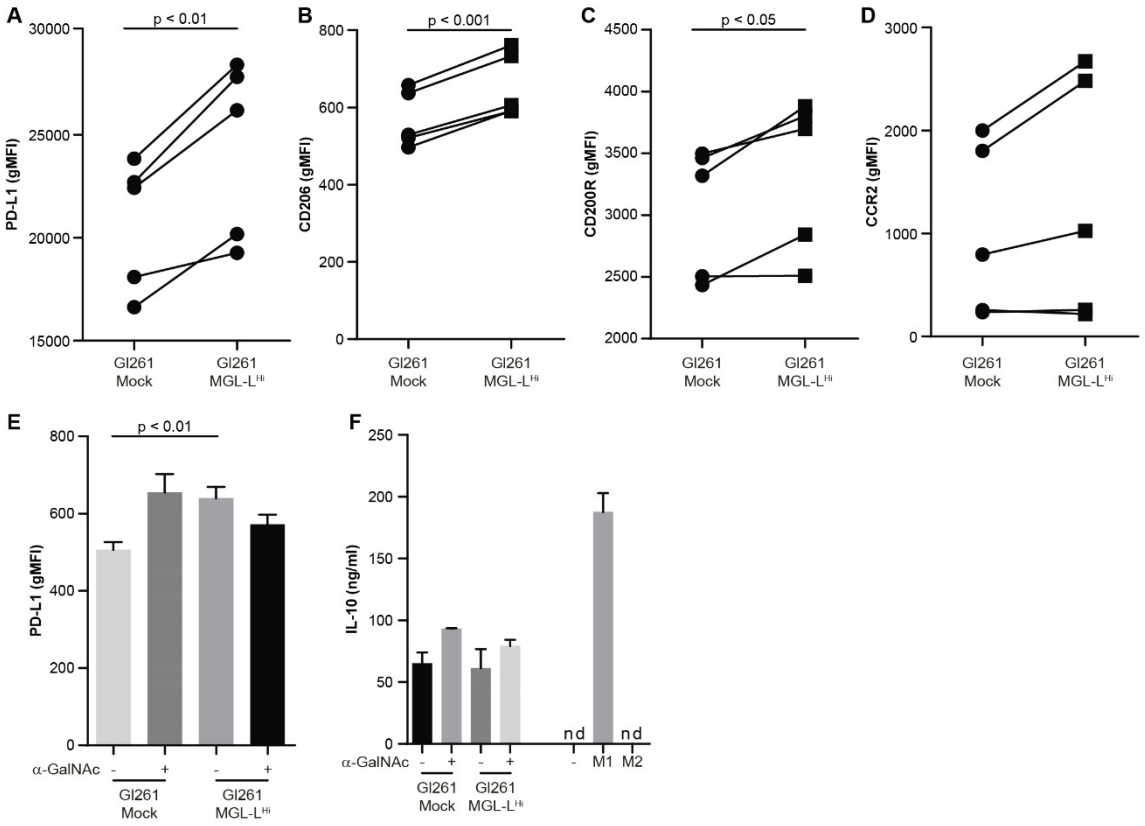

Fig. S4. ***In vitro*** **effect of the overexpression of glioblastoma MGL-ligands on macrophages and microglia.** Mouse peritoneal macrophages co-incubated with GL261 cells were assayed for the expression of PD-L1 (A), CD206 (B), CD200R (C), and CCR2 (D) by means of flow cytometry. Results indicate that the overexpression of MGL-ligands on the surface of the GL261 induces a significant increase in the expression of M2-like markers such as PD-L1, CD206, and CD200R. Co-incubation of the glioblastoma cell line GL261 with the microglia cell line BV-2 also resulted in an increase in the expression of PD-L1 on microglia (E) and the secretion of IL-10 (F). N=5, paired t-test.

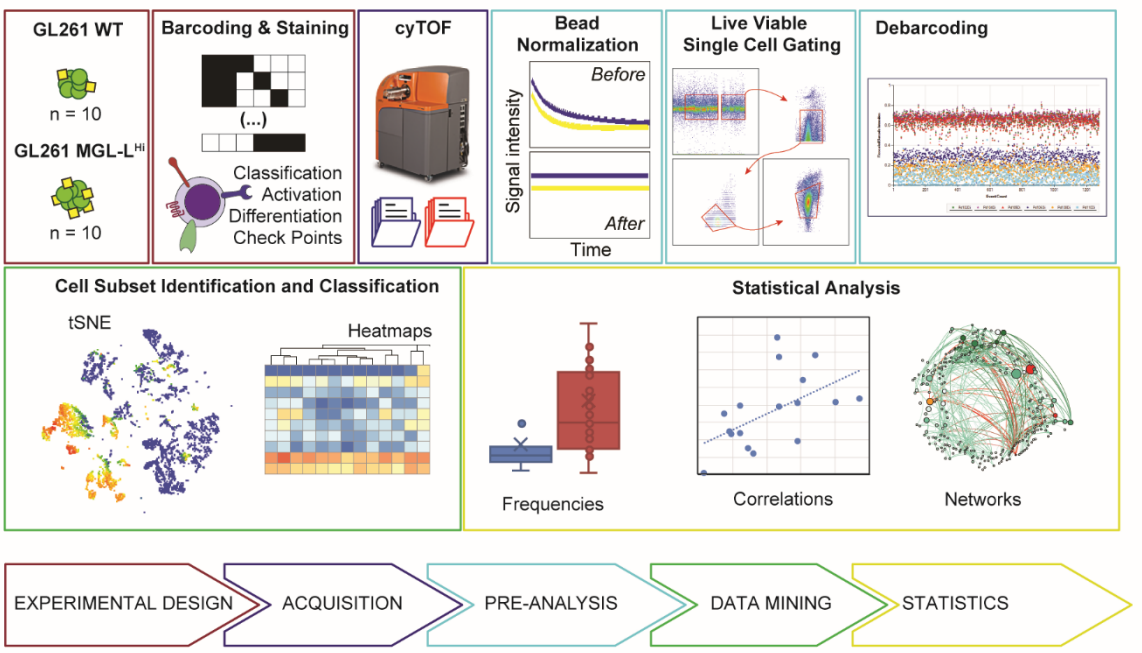

Fig. S5. Analysis pipeline. Our analysis pipeline starts with the experimental design including modification of the cell lines, design of the antibody panel, barcoding, and staining, followed by data acquisition on the mass cytometer. The pre-analysis starts with bead normalization, followed by manual gating of viable single cells, which then will be debarcoded. Next, we define cell clusters using HSNE (Cytosplore) and perform statistical analysis and network visualization.

Fig. S6. HSNE maps for all markers in the first HSNE level. HSNE maps, colour-coded for all the markers in the CyTOF panel, showing relative expression of the markers.

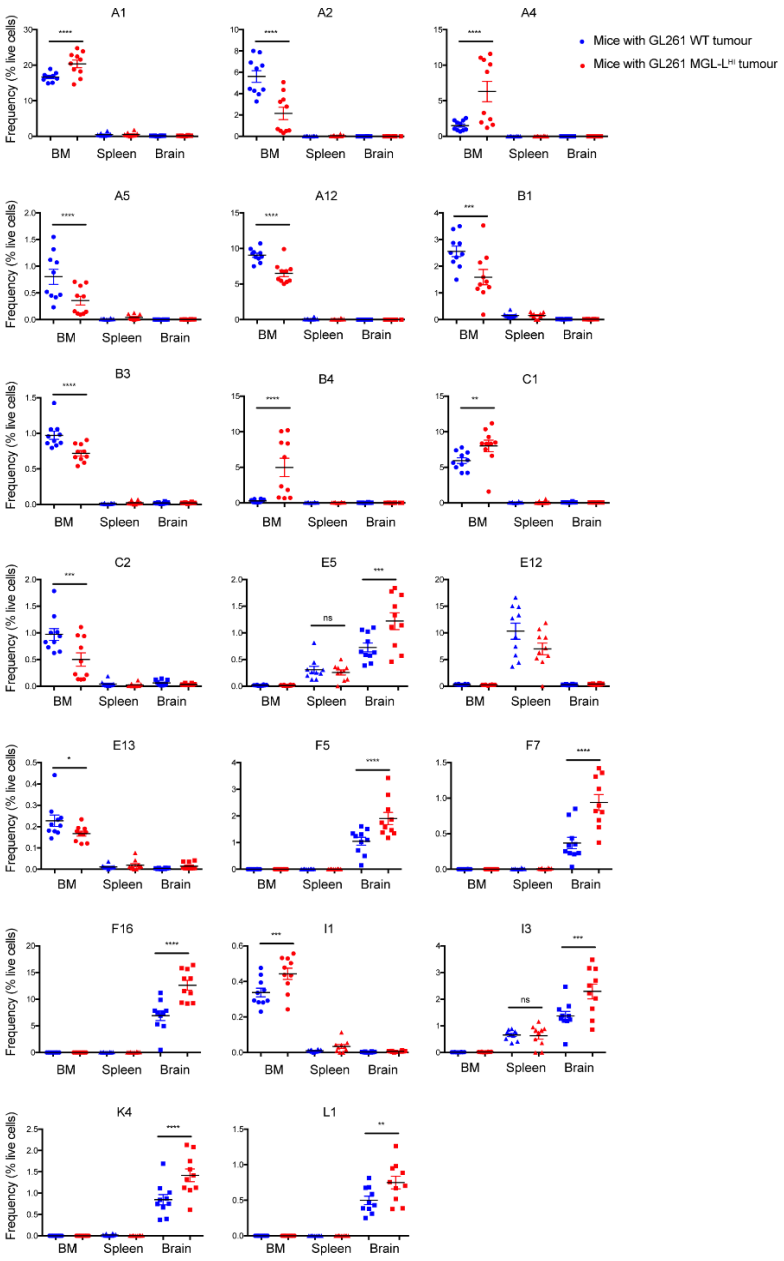

Fig. S7. Frequencies of clusters that contain statistically significant differences between WT and MGL-L^{hi} tumours. These graphs represent all the clusters with statistically significant differences in clusters between mice with WT or MGL-L^{hi} tumours. Differences were assessed with a one-way ANOVA test and post hock analysis looking at differences between clusters in the same organ, so WT brain versus MGL-L^{hi} brain, WT BM versus MGL-L^{hi} BM, and WT spleen versus MGL-L^{hi} spleen.

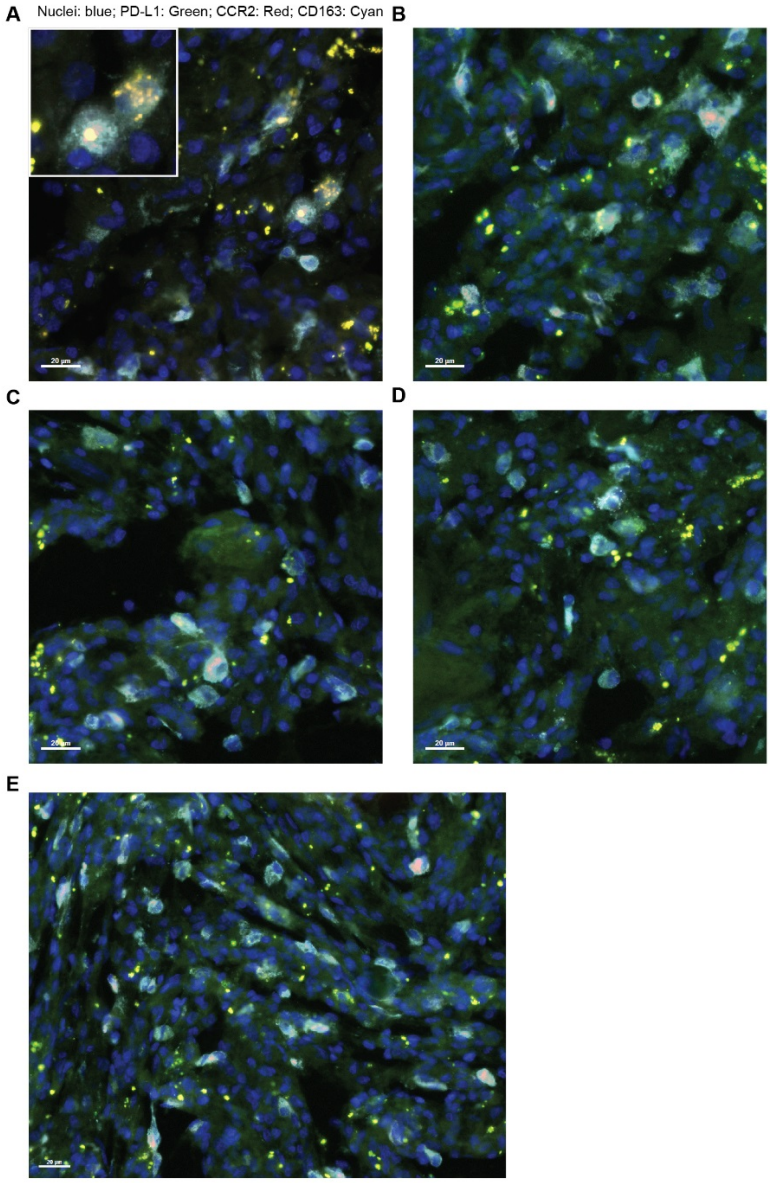

Fig. S8. Representative micrographs of tissues derived from glioblastoma patients. Tissues were stained with antibodies against PD-L1 (green), CCR2 (red), and CD163 (cyan). Nuclei were stained using the DNA dye DAPI (blue). A-E represent different fields and magnifications from the same tissue, clearly indicating a colocalization of PD-L1 and CCR2 on $CD163^{+}$ cells.

Table S1. List of 270 glycosylation-related genes.

A4GALT	B3GAT3	CHST11	EXT2	GALNS	GFPT1	HS3ST1	MAN2B1	NPL	SLC35A2	SULF2
A4GNT	B3GN-T6	CHST12	EXTL1	GALNT1	GFPT2	HS3ST2	MANBA	OGT	SLC35A3	TSTA3
ABO	B3GNT1	CHST13	EXTL2	GALNT10	GLA	HS3ST3A1	MFNG	PAPSS1	SLC35D1	UAP1
ALG1	B3GNT2	CHST14	EXTL3	GALNT11	GLB1	HS3ST3B1	MGAT1	PAPSS2	SLC35D2	UGCG
ALG10	B3GNT3	CHST2	FPGT	GALNT12	GLCE	HS3ST4	MGAT2	PGM1	ST3GAL1	UGCGL1
ALG10B	B3GNT4	CHST3	FUCA1	GALNT13	GMDS	HS3ST5	MGAT3	PIGA	ST3GAL2	UGCGL2
ALG11	B3GNT5	CHST4	FUT1	GALNT14	GMPPA	HS3ST6	MGAT4A	PIGB	ST3GAL3	UGDH
ALG12	B3GNT7	CHST5	FUT10	GALNT2	GMPPB	HS6ST1	MGAT4B	PIGC	ST3GAL4	UGP2
ALG13	B3GNT8	CHST6	FUT11	GALNT3	GNB1	HS6ST2	MGAT5	PIGH	ST3GAL5	UGT1A1
ALG14	B4GALNT1	CHST7	FUT2	GALNT4	GNB2L1	HS6ST3	MGAT5B	PIGM	ST3GAL6	UGT2A1
ALG2	B4GALNT2	CHST8	FUT3	GALNT5	GNE	HYAL1	MGC4655	PIGP	ST6GAL1	UGT2B10
ALG3	B4GALNT3	CHST9	FUT4	GALNT6	GNPDA1	HYAL2	MGEA5	PIGQ	ST6GAL2	UGT2B17
ALG5	B4GALNT4	CHSY1	FUT5	GALNT7	GNPNAT1	HYAL3	MPI	PMM1	ST6GALNAC1	UGT2B28
ALG6	B4GALT1	CHSY3	FUT6	GALNT8	GNS	HYAL4	NAGK	PMM2	ST6GALNAC2	UGT2B4
ALG8	B4GALT2	CMAS	FUT7	GALNT9	GPI	IDS	NAGLU	POFUT1	ST6GALNAC3	UGT8
ALG9	B4GALT3	CSGALNACT1	FUT8	GALNTL1	GUSB	IDUA	NANS	POFUT2	ST6GALNAC4	UST
B3GALNT1	B4GALT4	CSGALNACT2	FUT9	GALNTL2	GYLTL1B	KHK	NDST1	POMGNT1	ST6GALNAC5	UXS1
B3GALNT2	B4GALT5	CSGLCA-T	GAL3ST1	GALNTL4	HAS1	LARGE	NDST2	POMT1	ST6GALNAC6	WBSCR17
B3GALT1	B4GALT6	DAD1	GAL3ST2	GALNTL5	HAS2	LFNG	NDST3	POMT2	ST8SIA1	XYLT1
B3GALT2	B4GALT7	DDOST	GAL3ST3	GALT	HAS3	MAN1A1	NDST4	RENBP	ST8SIA2	XYLT2
B3GALT4	C1GALT1	DPAGT1	GAL3ST4	GBGT1	HK1	MAN1A2	NEU1	RFNG	ST8SIA3	
B3GALT5	C1GALT1C1	DPM1	GALE	GCNT1	HK3	MAN1B1	NEU2	RPN1	ST8SIA4	
B3GALT6	CHPF	DPM3	GALK1	GCNT2	HPSE	MAN1C1	NEU3	RPN2	ST8SIA5	
B3GAT1	CHST1	DSEL	GALK2	GCNT3	HPSE2	MAN2A1	NEU4	SGSH	ST8SIA6	
B3GAT2	CHST10	EXT1	GALNAC4S-6ST	GCNT4	HS2ST1	MAN2A2	NGALNAC-T2	SLC35A1	SULF1	

Table S2. Summary of antibodies used for CyTOF

Target protein	Clone	Metal	Source	Purpose
Cell identification				
Barcodes		103-110Pd	Fluidigm	Staining standardization & doublet discrimination
Iridium		191-193Ir	Fluidigm	Cell identification
Cisplatin		194-195Pt	Fluidigm	Live/dead discrimination
Cell classification				
CD45	30-F11	89Y	Fluidigm	All leukocytes
CD3e	145-2C11	152Sm	Fluidigm	T lymphocytes
TCRb	H57-597	169Tm	Fluidigm	T a/b lymphocyte receptor
CD4	RM4-5	145Nd	Fluidigm	T helper lymphocytes
Foxp3 (FJK16s)	FJK-16s	158Gd	Fluidigm	Regulatory T lymphocytes
CD8a	53-6.7	168Er	Fluidigm	Cytotoxic T lymphocytes
CD127 (IL-7Ra)	A7R34	175Lu	Fluidigm	Memory T lymphocytes
CD28	37,51	151Eu	Fluidigm	T lymphocytes, natural killer cells
Ly-6G/C (Gr-1)	RB6-8C5	141Pr	Fluidigm	Granulocytes
Ly-6C	HK1.4	150Nd	Fluidigm	Monocytes, macrophages
CD11b (Mac-1)	M1/70	148Nd	Fluidigm	Macrophages, microglia, dendritic cells, granulocytes
CD11c	N418	209Bi	Fluidigm	Dendritic cells
CD16/32	93	144Nd	Biolegend	Monocytes, macrophages
Tbet	4B10	161Dy	Fluidigm	T helper lymphocytes
CD5	53-7.3	146Nd	Fluidigm	Lymphocyte marker
CD49d	R1-2	176Yb	Biolegend	Exclusion marker for microglia
F4/80	BM8	156Gd	Biolegend	Dendritic cells, macrophages
CD62L (L-selectin)	MEL-14	160Gd	Biolegend	T lymphocytes
Siglec H	440c	166Er	Genetex	Plasmacytoid dendritic cells, Microglia
CD335 (NKp46)	29A1.4	153Eu	Fluidigm	Natural killer cells
aGFP	454505	173Yb	Biolegend	Tumor cells
CD36	No.72-1	147Sm	Fluidigm	Monocytes, macrophages, dendritic cells
CD19	6D5	149Sm	Fluidigm	B lymphocytes
Migration				
CCR2	475301	165Ho	RnD systems	Monocyte chemotaxis
CD185 (CXCR5)	L138D7	142Nd	Fluidigm	Lymphocyte chemotaxis
CD54 (ICAM-1)	YN1/1.7.4	163Dy	Fluidigm	Leukocyte extravasation
Activation				
Ly-6A/E (Sca-1)	D7	164Dy	Fluidigm	Hematopoietic stem cell marker/ activation of lymphocytes
Ki-67	B56	172Yb	Fluidigm	Cell proliferation
CD69	H1.2F3	143Nd	Fluidigm	Activated T lymphocytes
CD44	IM7	171Yb	Fluidigm	Activated lymphocytes
CD150 (SLAM, IPO-3)	TC15-12F12.2	167Er	Fluidigm	Activated lymphocytes and dendritic cells
CD154 (CD40L)	MR1	170Er	Fluidigm	Activated T lymphocytes
CD229	Ly9ab3	174Yb	Fluidigm	Activated lymphocytes and myeloid cells
Immune checkpoints				
CD152 (CTLA-4)	UC10-4B9	154Sm	Fluidigm	Co-inhibitory molecule
CD279 (PD-1)	J43	159Tb	Fluidigm	Co-inhibitory molecule
CD274 (PD-L1)	10F.9G2	155Gd	Biolegend	PD1 ligand
CD366 (Tim-3)	RMT3-23	162Dy	Fluidigm	Co-inhibitory molecule

Additional data S1

Summary according to the Author Checklist: MIFlowCyt-Compliant Items

Requirement	**Please Include Requested Information**
1.1. Purpose	Comparison of glioblastoma immune infiltrates and systemic immune status between mice with GL261-WT tumours and GL261-MGL-L^{HI} tumours
1.2. Keywords	Glioma, MGL, *O*-linked glycosylation, Tn antigen, Cosmc, C1galt1c1, Immune regulation, macrophages
1.3. Experiment variables	See antibody list supplementary table 2
1.4. Organization name and address	Amsterdam UMC, Vrije Universiteit Amsterdam, Dept. Molecular Cell Biology & Immunology, Amsterdam Infection & Immunity Institute and Cancer Center Amsterdam De Boelelaan 1117, 1081 HZ, Amsterdam, The Netherlands
1.5. Primary contact and email	Dr. Juan J. Garcia Vallejo, E-mail: jj.garciavallejo@amsterdamumc.nl
1.6. Date/time of experiment	October 2017
1.7. Conclusions	See main text manuscript
1.8. Quality control measures	See methods manuscript
2.1.1.1. Sample description	Single cell suspensions of brain, spleen and bone marrow
2.1.1.2. Source description	Mus musculus
2.1.1.3. Biological sample source organism description	Taxonomy: mus musculus; Gender: male; Age: 8-14 weeks Phenotype: WT; Treatment: intracranial glioblastoma (GL261) implantation
2.1.2.2. Environmental location	N/A
2.3. Sample treatment description	*See methods section of the manuscript* 1. Single cell preparation; 2. Cisplatin live/dead staining; 3. Barcoding and fixation; 4. Fc-receptor blocking; 5. Antibody cell surface staining; 6. Permeabilization and intracellular staining; 7. Iridium DNA intercalation
2.4. Fluorescence reagent(s)	N/A
3.1. Instrument manufacturer	Fluidigm
3.2. Instrument model	CyTOF 3 HELIOS
3.3. Instrument config./settings	See instrument settings table.

4.1. List-mode data files	FCS files have been deposited in Cytobank under file “Dusoswa et al. Glioblastomas exploit O-glycosylation – PNAS”
4.2. Compensation description	N/A
4.3. Data transformation details	ArcSinH(5)-transformation in Cytobank
4.4.1. Gate description	Live single cells were gated before analysis in Cytosplore
4.4.2. Gate statistics	N/A
4.4.3. Gate boundaries	N/A